CrossMark

ORIGINAL PAPER

Geophysical surveys for identifying source and pathways of subsurface water inflow at the Bangur chromite mine, Odisha, India

Arkoprovo Biswas[1,2] (iD) · Shashi Prakash Sharma[2]

Abstract Geophysical survey was carried out in an effort to solve an underground flooding problem at the Bangur chromite mine of Odisha Mining Corporation Limited, Odisha, India. To identify sources and pathways of the influx, very low-frequency electromagnetic, self-potential and resistivity surveys were performed. Geophysical studies clearly depict a major fracture zone passing through the mine and its connection to a water storage pond. The fracture zone extends further west from the pond to the Salandi River and the Salandi Reservoir. The dip of the delineated fracture zone is around 45° to the N, and it matches with the fault plane exposed in the mine. Since water enters into the mine from the west, the delineated fracture zone is thought to be the main pathway for the inflow. Geophysical studies conclude that the IMFA pond, Salandi River and Salandi Reservoir could be possible sources of water in the mine. To ascertain the source and pathway, tracer testing was conducted at two locations, based on the geophysical survey by the hydrogeological team, but tracer test results were inconclusive. However, the fact remains that the water enters to the mine through the delineated fracture and poses threat in mine operation. Dumping water in nearby pond will again enter in mine with interconnected fractures. Therefore, for safe mining operation, it is proposed to drill a slanted tube well at the delineated fracture and pump out maximum water and discharge the pumped water at canal situated about 2.5 km from the mine.

Keywords Underground mining · Water influx · Fractures · VLF-EM · Resistivity · SP anomaly

✉ Arkoprovo Biswas
  arkoprovo@gmail.com

  Shashi Prakash Sharma
  spsharma@gg.iitkgp.ernet.in

[1] Wadia Institute of Himalayan Geology, 33, G. M. S. Road, Dehradun 248001, Uttarakhand, India

[2] Department of Geology and Geophysics, Indian Institute of Technology Kharagpur, Kharagpur, W.B. 721302, India

 Springer

1 Introduction

Underground mining activities are associated with hazards such as underground flooding, roof collapse and wall collapse. Sudden inflows of water into underground mines have resulted in thousands of causalities (Vutukuri and Singh 1995). Intense leakage of groundwater into underground mines has long been a very serious problem for the mining industry (Jakubick et al. 2002; Nuttall and Younger 2004; Ricka et al. 2010; Sui et al. 2011). A number of accidents have been reported worldwide relating to flooding and seepage of surface and subsurface water in underground mines (Moebs and Sames 1989). Mining under complex hydrogeological conditions can be dangerous and extremely costly. Precise prediction and forecasting of subsurface mine leakage is challenging, and appropriate remediation measures need to be implemented. The ever-increasing depth of mines results in a significant increase of groundwater inrush from the underlying aquifers. Dewatering and discharging of water from nearby ponds or water reservoirs is also dangerous if they are connected to the mine by fractures (Wanfang 1997). In many countries, there are guidelines for subsurface mine flooding (Landerarbeitsgemeinschaft Wasser [LAWA] 2001). Besides this, many other processes to prevent subsurface mine flooding have been reported (Klapper et al. 1996).

   The Sukinda thrust zone at the junction of the Singhbhum granite and the Eastern Ghat Mobile Belt is an important source of chromite deposits in India (Fig. 1, left panel). A number of opencast and underground chromite mines operate in this region. Being a thrust zone, the area is characterized by a number of faults systems. Furthermore, as this is a monsoon-dominant region and adjacent to a coastal zone, it has several rivers and reservoirs. Hence, plenty of groundwater moves through the complex fracture system in the area. Unfortunately, the Bangur chromite mine encounters such a fracture (Fig. 1, right
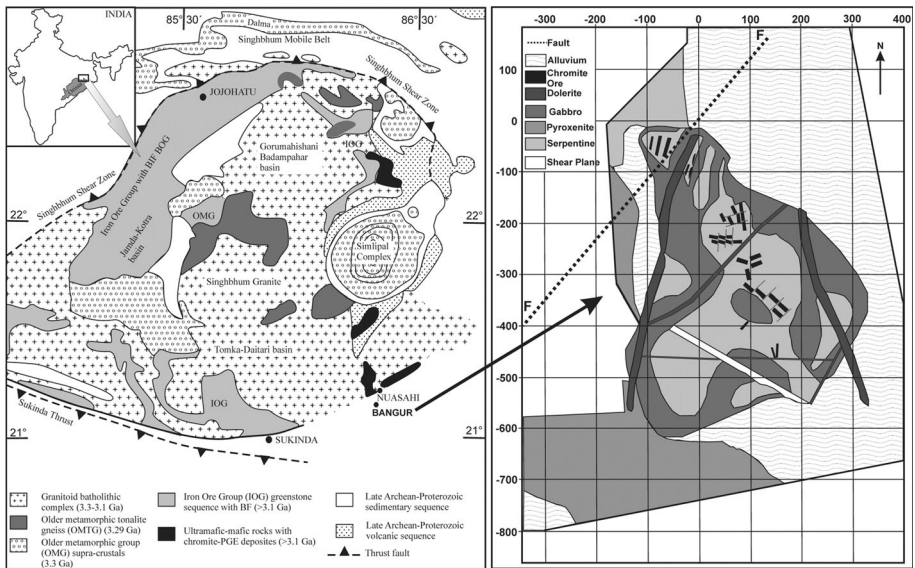

Fig. 1 Regional geological map (*left panel*-modified after Saha 1994; Mohanty et al. 2011) and geological map of OMC chromite mine (*right panel*-Pers. comm., OMC)
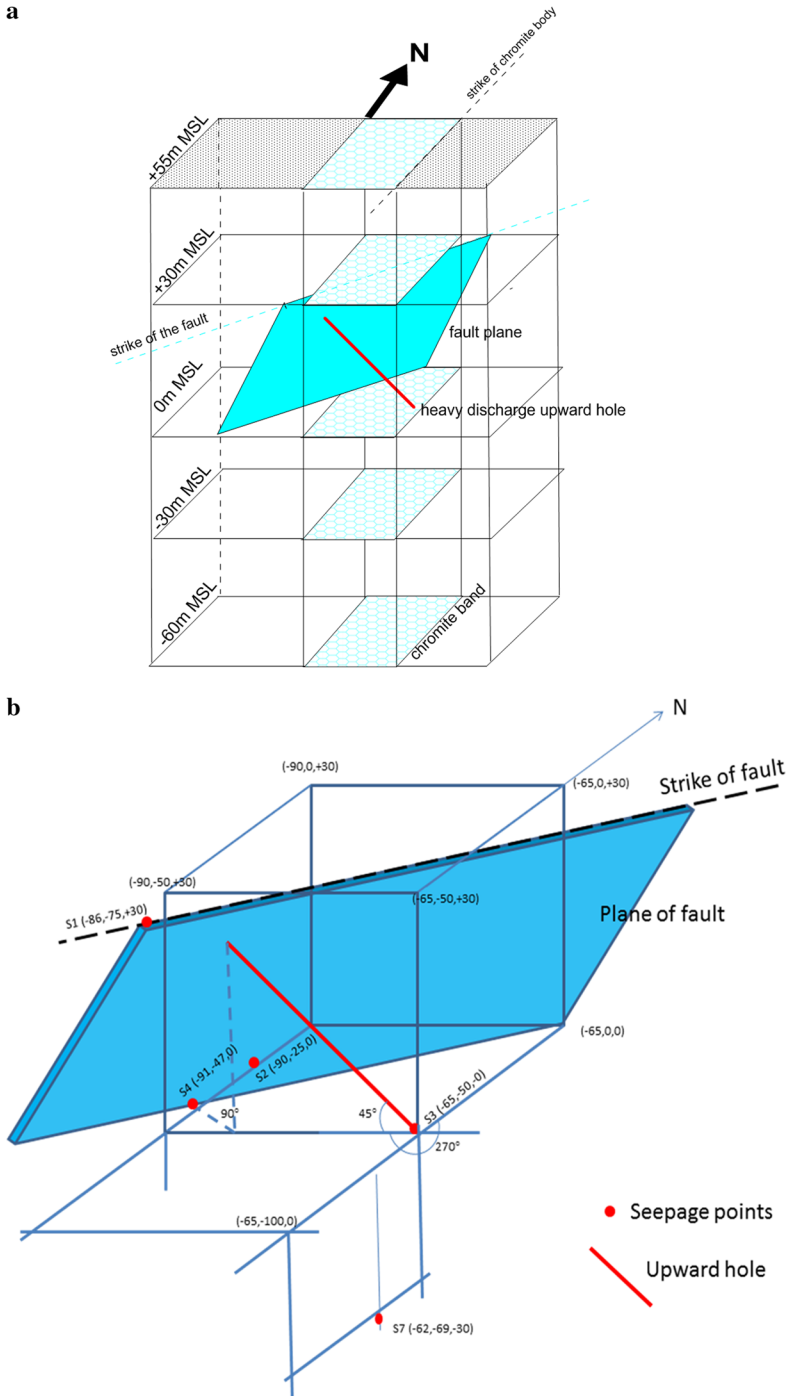
a

b

Fig. 2 a Schematic diagrams of various levels in OMC underground mine. *Inclined blue shading* is the fault plane. *MSL* mean sea level. **b** A 3-D view of location of seepage from various levels in local coordinate

panel). Figure 2a depicts a schematic diagram with various levels in the mine, the fault plane, the strike of the fault, as well as the dip and location of an upward-drilled borehole. Figure 2b shows the locations of water seepage in the mine (red circle) in local coordinates. The thick red line shows substantial water flow through the borehole. A profuse discharge of water has been encountered in this borehole, which together with several other discharges at different levels causes flooding in the mine. This flooding hampers mining and poses a risk to personnel working in the mine. The mean seepage rate at each point is listed in Table 1.

From the present scenario, the Odisha Mining Corporation (OMC) Limited pond (an abandoned open chromite pit), the Indian Metals and Ferro Alloys (IMFA) pond (another abandoned open chromite pit), the Salandi River and the Salandi Reservoir are the most probable sources of seepage into the mine. Moreover, natural groundwater present in the area might also be a source of water influx into the mine. Fractured aquifers, fracture zones, dykes and fault planes were often seen with chromite deposits within the OMC mine. An integrated geophysical survey using very low-frequency (VLF) electromagnetic, resistivity and self-potential (SP) methods (Sharma and Baranwal 2005; Sharma et al. 2014) was applied to map the fracture zones. A VLF electromagnetic, resistivity and SP survey was carried out near the mine to investigate the potential sources and to define an appropriate dewatering mechanism for continuous trouble-free and safe mining activity. To achieve our objectives, we conducted geophysical surveys using the above-mentioned methods and hydrogeological investigations such as tracer test.

2 Regional geology and hydrogeology

2.1 Geology and structure

The area is situated in the southern part of the exposed Baula–Nuasahi ultramafic complex (Fig. 1, left panel). The ultramafic complex strikes in the NNW–SSE direction, dipping at 75°–80° towards the NE, and is characterized by chromite-bearing ultrabasic rocks and gabbro–anorthosites (Pers. comm., OMC; Sahoo et al. 2014). The whole ultramafic complex bears an intrusive relationship with iron ore group (IOG) rocks and lies un-conformably on a sequence of meta-sediments, in addition to being invaded by dykes of a younger, dolerite group. The major structure of the area has been described by Banerjee (1972) as a south-westerly plunging syncline, the northern limb of which is hidden under laterite and soil. The various sets of minor rolls on the limb indicate a major synclinal fold. An east–west trending fault runs along the major fold. The chromite occurs in disconnected, lensoid bands trending north–south on the southern part of the area and NNW–SSE in the northern part, conforming to the general foliation of the

Table 1 Mean seepage rate at various points as mentioned in Fig. 2b (Pers. Comm. OMC)

Level (MRL)	Point No.	Seepage of water
+30	S1	1440 L/h
0	S2	156 L/h
0	S3	12 L/h
0	S4	16,200 L/h

country rocks. The general strike of the basic rock is N55°W and the dip is almost sub-vertical, as revealed in the sectional study. Within the basic rock, spotted chromite bodies are found as floats, which imply that the basic rocks intruded later than the ultrabasic rocks. Minor faults and drag folds are also visible in the quarry exposures. Numerous minor slips with well-marked slickensides are geo-technically significant structural features in the wall rocks. The rocks are highly jointed and fractured. Three sets of joints are also found at different places in the dolerite, gabbro and serpentinites, which are fine-grained altered products of peridotite–dunite suite rocks. Various oblique and vertical joints are very common. The mineralization, as evidenced from the field study, is mainly controlled by lithology and structure. A geological map of the study area is shown in Fig. 1 (right panel).

2.2 Hydrogeology, geomorphology and water quality

The Bangur chromite mine area is characterized by an overall gently sloping topography, with an overall ground slope towards the south. The highest elevation point is 86 MRL (mean reduced level) at the northern part of the mine, and the lowest point is at 46 MRL in the southern part (Pers. comm., OMC). The whole area near the mine exposes a sub-dendritic, low-density drainage pattern. The Salandi River is the principal drainage channel in the area, collecting the surface run-off from all its tributaries, distributaries and seasonal streamlets from the hills. The Salandi River is a non-perennial river, approximately 2.5 km to the west of the mine and flowing towards south. The humidity and temperature are typical for a tropical area. Annual rainfall in this area is of the order of 1500–1600 mm/year (Pers. comm., OMC).

There are three distinct physiographic landforms marked in the mine area. The north-eastern hill slopes are mainly covered with colluvial soil and scree, consisting of rounded rock boulders of mostly basic gabbroic composition. This part is mostly a degraded forestland with sparsely distributed bushy overgrowth. Intermediate plain land is covered by soil. Both the western and eastern flanks of the mine area are covered by this landform and used mainly for agriculture and farming purposes. The chromite deposits in the south-eastern part of the mine area are hosted by this category of land. The southern highland consists of laterites, originating from the resistant basic parentage. This landform usually has poor vegetation cover, except for sporadic trees and bushes of ipomea. Small amoeboid chromite bodies are occasionally found within the laterite deposits. The depth of laterite varies from 8 to 25 m (Pers. comm., OMC).

The water quality analysis (after Dhal et al. 2011) such as pH, temperature, electrical conductivity (EC), total alkalinity (TA), total solids (TS), total suspended solids (TSS), total dissolved solids (TDS), total hardness (TH) and total chromium is shown in Table 2.

3 Methodology

Delineation of the fracture zone (exact location and orientation) can be done using resistivity and electromagnetic surveys. Since a resistivity survey was not possible within the premises of the Bangur mine, due to subsurface cavities, exposed hard rock and dumping of chromite on the surface, a VLF electromagnetic survey was conducted there. Since the primary hypothesis was that the source of the groundwater in the mine was the IMFA and OMC ponds VLF, resistivity and SP measurements were recorded parallel to the

Table 2 Water quality analysis of OMC (after Dhal et al. 2011)

Sl. no.	Parameters	Range	Indian standards
1	pH	5.94–6.32	6.5–8.5
2	Temperature (°C)	26–28	30
3	Conductivity (mS/cm)	750–1110	–
4	Total alkalinity (TA) (mg/L)	132–210	300
5	Total solids (TS) (mg/L)	630–1043	600
6	Total suspended solids (TSS) (mg/L)	12–64	100
7	Total dissolved solids (TDS) (mg/L)	534–946	500
8	Total hardness (TH) (mg/L)	258–305	300
9	Total chromium (mg/L)	0.76–1.25	2

edge of the IMFA pond. Subsequently, VLF profiles were taken on the basis of previous profiles to trace the direction of the fault whether it is connected to other natural source such as the Salandi River and the Salandi Reservoir.

3.1 Very low-frequency (VLF) electromagnetic survey

The VLF method is a semi-passive electromagnetic induction method that utilizes distant high-power vertical radio transmitters as a source for its primary field. These transmitters are meant for long-distance marine communication and located in coastal areas worldwide. They operate in the lower band (5–30 kHz) of communication frequency. These signals travel a long distance and can be used for geophysical measurements several thousand kilometres away from the transmitters. Since the primary field is horizontal, the VLF method is ideal for the investigation of vertical and dipping conducting structures in the subsurface, such as the nearly vertical subsurface structures in the area (Sharma et al. 2014; Biswas and Sharma 2015).

The measurements were taken using an ABEM Wadi VLF instrument that detects magnetic field components. The instrument measures the ratio of the vertical component of the magnetic field (Hz), which depends on the subsurface conductor, and the horizontal component of the magnetic field (Hx), which mostly depends on the VLF transmitter. The ratio (Hz/Hx) yields the tilt angle and ellipticity and can be converted into a real and an imaginary VLF anomaly (Sharma et al. 2014; Biswas and Sharma 2015). The strike of the formation is approximately in the E–W direction; hence, a transmitter in the E–W direction with a frequency 19.8 kHz was selected for E-polarization measurements. Subsequently, VLF data were collected along N–S profiles with a 10-m station interval. The measured real and imaginary anomalies could be converted into apparent current densities using Karous and Hjelt (1983) filtering technique. The expression for the filtering technique is given as:

$$\frac{\Delta z}{2\pi} I_a(0) = -0.102 H_{-3} + 0.059 H_{-2} - 0.561 H_{-1} + 0.561 H_1 - 0.059 H_2 + 0.102 H_3 \quad (1)$$

where $I_a(0) = 0.5[I(\Delta x/2) + I(-\Delta x/2)]$, which is the equivalent current density value. This filter is calculated and applied on equal-spaced data with the hypothesis that the transformed current density values correspond to the depth Δz, which is equal to the data

spacing at which the current densities are to be calculated (Sharma et al. 2014). Δx is the data interval, and the relation between the data interval and the pseudo-depth is a not a mathematical relationship but a convention only. The mathematical derivation can be found in Karous and Hjelt (1983) and is not discussed here for brevity. The processing and generation of VLF real and imaginary anomalies and the subsurface current densities were carried out according to Sharma et al. (2014). The 2-D depth section represented by low (blue) and high (red) current density values simulates resistive and conductive features, respectively. Resistive features can be correlated with non-metallic rock, e.g. host rock gabbro or dolerite dykes. Conductive features are correlated with metallic chromite bodies or fractures filled with groundwater. For VLF profiles, it should be mentioned that due to mining activities, high-power transmission lines are present in those areas. Hence, it is unlikely to do VLF survey in a regular pattern of profile of equal length and spacing.

3.2 Self-potential (SP) survey

Groundwater movement through fractures is characterized by small positive self-potential anomalies (Sharma and Baranwal 2005) or streaming potentials. Therefore, SP measurements were taken along a profile to depict such zones. Non-polarizable Cu-CuSO$_4$ electrodes were used, and measurements were taken with 0.1 mV accuracy. For self-potential measurements, the distance between the potential electrodes was 10 m. Since self-potential associated with massive mineralization, disseminated mineralization, contact zone and zones associated with groundwater movement are different, SP measurements will provide the characteristics of the subsurface in the area.

3.3 Resistivity profiling

Resistivity profiling is suitable for depicting lateral variations in the resistivity of the subsurface. Resistivity profiling using a Wenner–Schlumberger array (Telford et al. 1990) was carried out along VLF profile P1 to confirm the nature of the structure (Fig. 3) depicted in the VLF data. Wenner–Schlumberger array has good signal strength and high lateral resolution over other electrical arrays and is mainly used to detect narrow and vertical structures (Telford et al. 1990). This array is more suitable for mapping thin structures at depth compared to conventional Wenner array (Telford et al. 1990). Further, this array is better in terms of signal strength compared to gradient profiling where current electrodes are placed at a large distance and potential electrodes are moved in the central part of the profile (Telford et al. 1990). Looking at the depth of problematic zone in the mine, we expected information up to 30 m depth at high lateral resolution. Therefore, we fixed the distance between outer electrodes C1–P1 and C2–P2 as 50 m and inner electrodes, that is, P1–P2 as 10 m and moved whole array along the profile at 10-m interval. This way we got good signal strength and good lateral resolution. The distance between the two potential electrodes 'b' was 10 m, and the current electrodes were positioned 50 m from the potential electrodes 'a' on either side (Fig. 4). The depth of penetration for resistivity measurements depends on the total length of the current electrode, i.e. distance between C1 and C2 is about 1/3rd to 1/4th of the current electrode spacing. Since in the present work the distance between C1 and C2 is 110 m, the depth of penetration is around 30 m which is sufficient enough to detect the fault plane situated at a depth of 25 m below the surface. Moreover, the whole array was moved at an interval of 10 m till 220 m and the centre of the array is considered as the point of observation. The expression for apparent resistivity (ρ_α) can be written as:
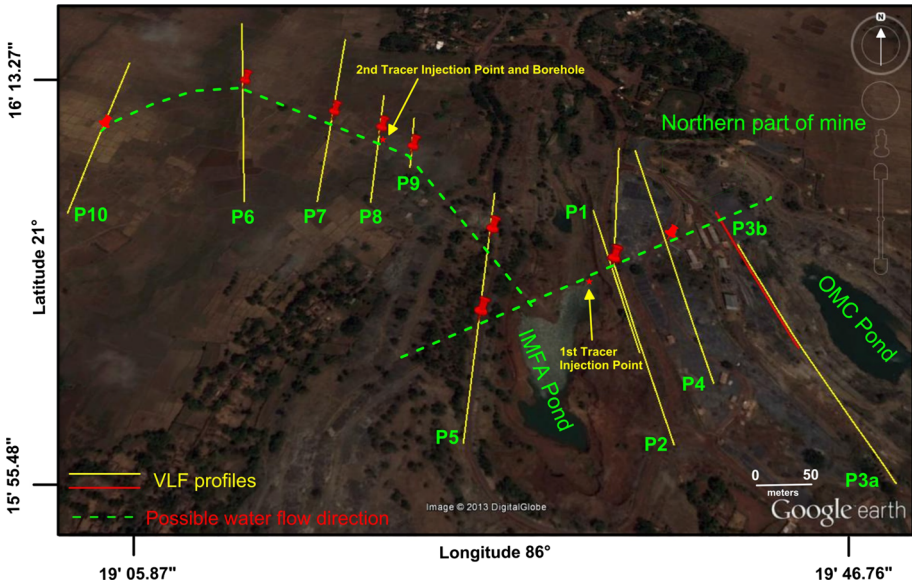
Fig. 3 Location of the geophysical survey profiles (VLF, SP and resistivity), tracer injection points and borehole location on the Google image of the study area. *Red blobs* are the position of the fracture zone from where it is connected
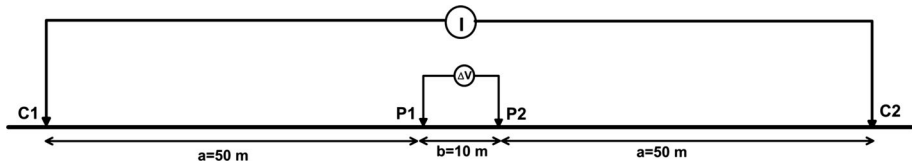

Fig. 4 Electrode configuration for Wenner-Schlumberger array (Telford et al. 1990)

$$\rho_a = \pi \frac{a(a + b)}{b}\left(\frac{\Delta V}{I}\right) \tag{2}$$

where ΔV is the potential difference between potential electrodes and I is the current flow in the subsurface. Since the signal strength (potential difference) is quite small, very precise cancellation of self-potential is required. The whole arrangement of electrodes is moved along the profile, and the centre of the array is considered as the point of observation. The apparent resistivity can be plotted to know the subsurface structure at appropriate depth. It is also important to mention that even though the maximum discharge is at 0 MRL, the source of water is at a much higher level. When OMC drilled a 45° tilted hole in vertical direction, it punctured at the fault zone and water started gushing out in the bore whole. So the actual source of water is much above than 0 MRL. Hence, from the above configuration of Wenner–Schlumberger array, 110 m C1–C2 distance is able to see the same fracture.

3.4 Tracer test

Groundwater movement in the subsurface can be delineated using tracer test techniques. Conservative tracers are used to evaluate effective porosity and dispersivity. Aqueous solutions of halides were used to delineate the subsurface flow from the IMFA pond to the Bangur mine. The approximate size of the IMFA pond is 300 m × 100 m × 10 m. The concentration of the halide tracer is only affected by inflow dilution. It was anticipated that, given the mass of the halide used, even after being diluted by the volume of water estimated to be hypothetically flowing through the discontinuity, it could be detected in the downstream seepage points if it were connected. The salient features of the test are mentioned below as conducted by other team (personal communication, Dr. A. Mukherjee, IIT Kharagpur).

A fluorescent dye was used as a visual tracer to delineate the tracer plume and also as a semi-conservative tracer test. Fluorescent dyes have been used in conservative stream-tracking studies. However, they seem to decay over time. The tracer solution was made by dissolving 15 kg of visual dye and 100 kg of halide salt in 2000 L of water. The solution was thoroughly stirred to ensure homogeneity. Next, the solution was pumped into the delineated fracture zones at IMFA pond (Fig. 3), assuming that there was conduit connectivity between the IMFA pond and the seepage points in the Bangur chromite mine. Another tracer test was performed at a drilled borehole based on the geophysical survey.

4 Results and discussion

VLF electromagnetic, resistivity, self-potential as well as hydrogeological studies were carried out to understand the source of water in the Bangur chromite mine. The results of the geophysical survey, as it progressed, are presented step by step below:
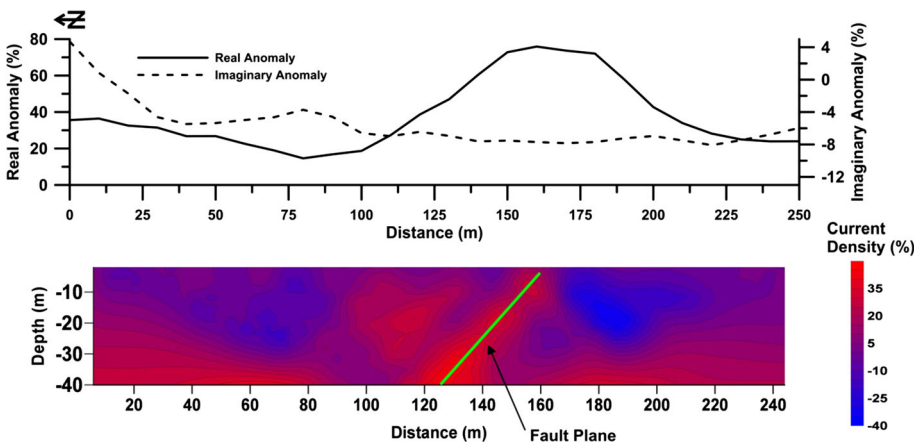

Fig. 5 VLF anomaly (real and imaginary) along profile P1 and the corresponding current density section. *Green line* represents the fault/fracture zone

4.1 Profile P1 (VLF profile)

Profile P1 (Fig. 3) is the first VLF profile, and it was carried out in the N–S direction. Figure 5 depicts the real and imaginary anomalies, and the apparent current densities computed using real anomalies. The data show a fracture zone passing through location 130 m (approximately 45°N and has a strike of W20°S–E20°N direction), dipping in a northerly direction at an angle of 45°. This location coincides with the northern edge of the IMFA pond. The dip of the delineated fracture correlated very well with the fracture seen in the underground mine at 0 MRL. Therefore, the fracture on this profile near the IMFA pond was interpreted as continuing in the mine. Under such circumstances, if the IMFA pond is filled with water (either rain water or storage water from the nearby mine), then water may percolate through this fracture and flow into the mine. This geophysical finding is validated with a tracer test to determine whether water from the IMFA pond enters the mine or whether the depicted fracture is connected with some other water source.

Before starting the hydrogeological test, the VLF survey was repeated in the opposite (S–N) direction to check that the same fracture zone could be detected using the reverse direction of the VLF profile. Resistivity and self-potential data were also measured to pinpoint the exact location of the fracture zone. A substantial correlation was observed between the delineated fracture near the IMFA pond and the fracture seen in the mine, after a tracer test was conducted in the IMFA pond. The tracer was pumped into the nearest point where the fracture is intersecting the pond (Fig. 3) and it diffused into the large volume of water at IMFA pond.

4.2 Profile P2 (VLF, resistivity and self-potential)

VLF profile P2 was conducted from the south to north direction. Figure 6a depicts the measured real and imaginary anomalies and the interpreted vertical current density cross section (Fig. 6b). A dipping conductive structure (fault/fracture) can be seen at 150 m along the profile. This indicates that a fracture is present at this location. High current density depicted at the southern part of the profile at 250–300 m is associated with a chromite deposit which is also visible at the surface. The VLF measurements along profiles P1 and P2 were taken at a time interval of almost 4 months. However, computed current densities for both profiles clearly depict the same fracture zone along the same dip and direction.

Electrical resistivity profiling and self-potential measurements were also carried out along profile P2, for correlation with the VLF measurements and to precisely locate the fracture location, since maximum discharge of water in the mine was seen to occur at 0 MRL (50 m below ground level). Wenner–Schlumberger profiling measurement was taken to pick up the appropriate signal. Since the signals associated with the subsurface structure are very weak, we used this array because of its excellent signal strength and high sensitivity. Figure 6c depicts a 220-m-long resistivity profile. At 120 m, a highly resistive structure (dolerite dyke) was observed. A conducting structure observed at 150 m correlated well with the VLF observation along profiles P1 and P2. Since the main interest was the conductive structure, data representing the dolerite dyke were discarded and plotted again. The data refinement better revealed the drop in apparent resistivity due to a possible fracture zone, compared to surrounding rocks. This data refinement was particularly applied because of the effect of dolerite dyke on the fault plane. To examine the exact anomaly generated due to fault and the fluid movement within the fault plane, both resistivity and SP data were recalculated negating the effect of dolerite dyke.
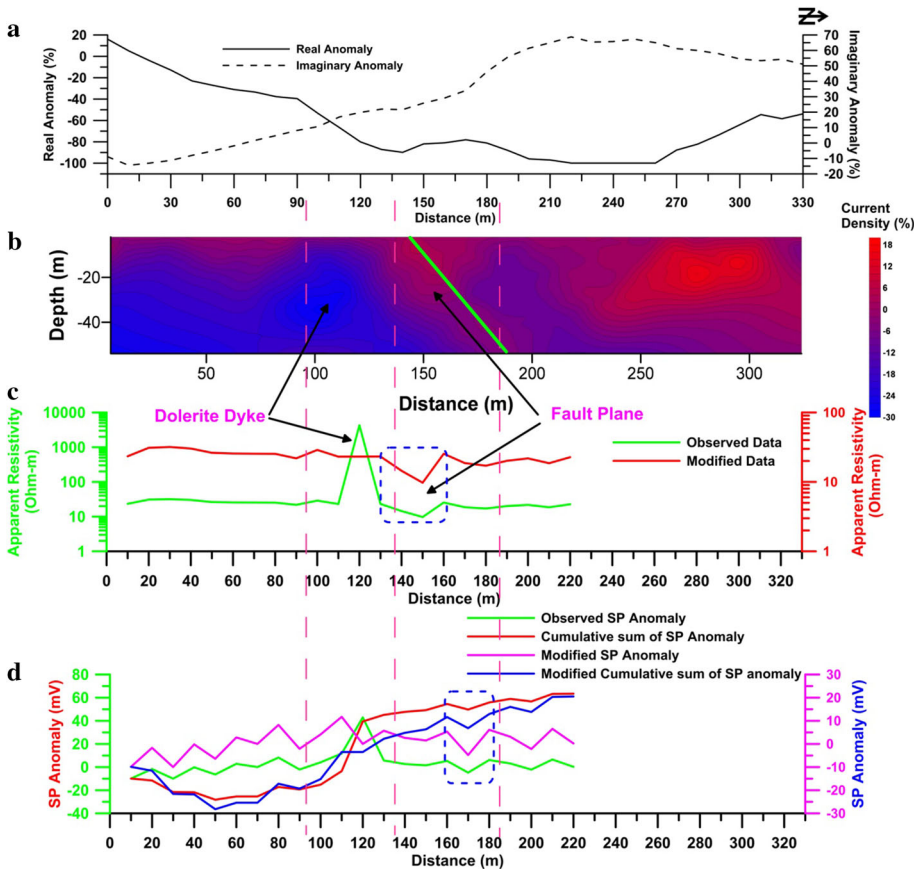
Fig. 6 **a** VLF real and imaginary anomaly, **b** current density section, *green line* shows the fault plane.
c Resistivity profile, **d** self-potential anomaly

A self-potential anomaly (Fig. 6d) is also present at the expected fracture location, characterized by an increased signal at 120 m. This peak signal corresponded to a resistive structure (dolerite dyke) and can therefore be interpreted as contact potential. This contact potential value was taken as background SP (0 mV), and the modified self-potential anomaly was calculated. The modified anomaly shows a typical SP anomaly due to a fault-type structure at 160–180 m. Moreover, the absence of a significant positive high or low SP anomaly exactly over the fracture could indicate water flows at depth. As it is known that water enters the Bangur mine through this fracture zone, it can be argued that flow at a depth of 30 m might not produce an SP anomaly that is significant enough for detection at the surface.

4.3 Profiles P3a and 3b (VLF profile)

Profiles 3a and 3b were taken on the western side of the OMC pond (Fig. 3) to locate possible fractures in this direction. Even though water seepage in the underground mine could not be observed from the south-eastern direction of the OMC pond, VLF

measurements were also taken on a profile. Figure 7a depicts the measured VLF anomalies and interpreted depth section. The alternating resistive and conducting features reveal a conducting chromite body and resistive host along this profile. No thin fracture or conducting fault-type structure is seen on this profile. This is in accordance with the direction of seepage observed in the OMC mine.

Profile 3b was taken to cover a part of profile P3a and extended north to the premises of the mine (Fig. 3—red line). The VLF anomalies and current density sections are shown in Fig. 7b. A resistive feature representing a dolerite dyke is seen at around 90 m on this profile. Conducting features representing chromite bodies are seen after the dolerite dyke, but the major fracture is not seen on this profile. This signature was also observed at the surface where the dolerite dyke passes into the mine. Since a fracture is known to be present under this profile, the data should have indicated its existence. The reason for the missing fracture anomaly could be the noisy environment, voids inside the mine or an
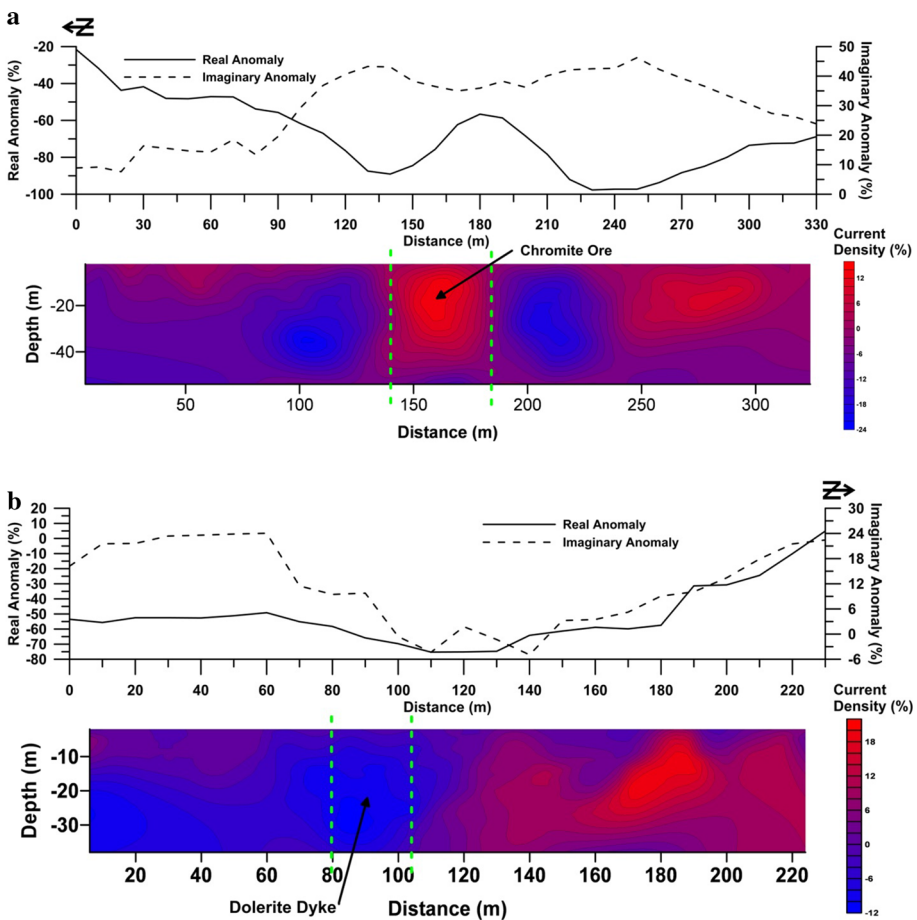

Fig. 7 **a** VLF anomaly (real and imaginary) along profile P 3a and the corresponding current density section. Chromite ore deposit is shown by the *dotted green line* within two resistive host rocks. **b** VLF anomaly (real and imaginary) along profile P 3b and current density section. *Dotted green line* shows the dolerite dyke

unsaturated fracture. It can also be argued that the upper part of the fracture was not saturated with water, as water was moving down into the mine.

4.4 Profile P4 (VLF profile)

Profile P4 was conducted between profiles P1 and P3 to depict the location of the fracture (conductor) seen on profile P1 near the IMFA pond (Fig. 3). The recorded data were quite noisy due to a chromite dump as well as some electrical cables and buildings (Fig. 3) in this area. A resistive structure seen at a distance of about 240 m on this profile is a dolerite dyke. A shallow conductor is seen on this profile at a location of nearly 300 m (Fig. 8). This structure is correlated with the northward dipping fracture on profile P2.

Interpretation of the VLF anomalies of the profiles between the OMC mine and the IMFA pond led us to conclude that the IMFA pond is a possible source of water seepage in the OMC mine. Hence, a hydrogeological tracer test was executed at this location to check whether there is any seepage from the fracture zones. Prior to this, electrical resistivity and self-potential measurements were performed and correlated with VLF measurements along VLF profile P2 to precisely pinpoint the location for the tracer test in the IMFA pond.

4.5 Profile P5 (VLF profile)

VLF measurements were further taken along profile P5 adjacent to the western side of the IMFA pond in a S–N direction to see whether the fracture further extends beyond the IMFA pond. Figure 9 depicts the recorded VLF data and current density section. The northerly dipping high current density (red) zone between 150 and 200 m is the same fracture which was observed on the eastern side of the IMFA pond on profiles P1 and P2. This means that the fracture in the mine has a long extension towards the west. On this profile, two fractures were seen. One was the extension of the fracture in the mine seen on the east side of the IMFA pond (between 150 and 200 m), and the other one was further north of the first fracture (320 m location). A resistive feature was also seen on this profile near 100 m, which was possibly the dolerite dyke.
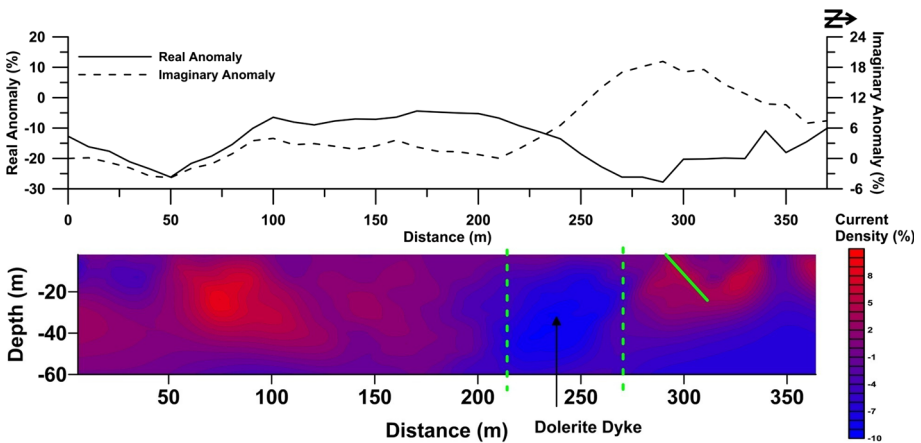

Fig. 8 VLF anomaly (real and imaginary) along profile P4 and current density section. Dolerite dyke is shown by *dotted green line* and fault/fracture plane is shown by *solid green line*
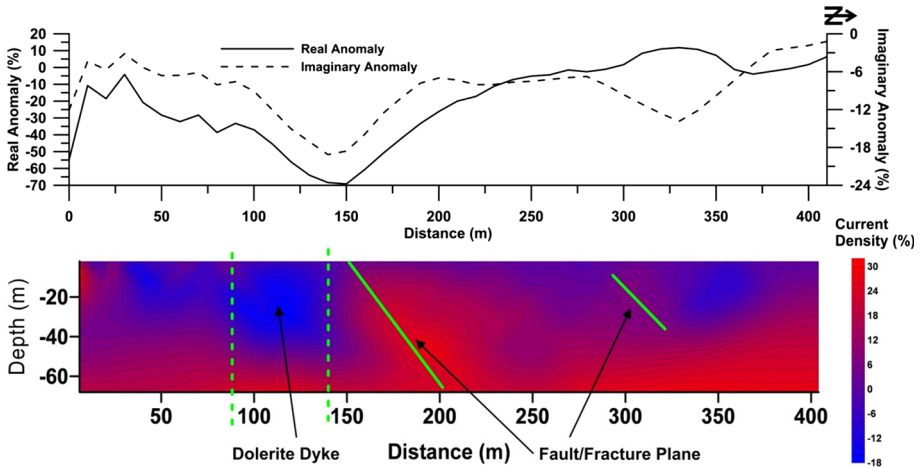
Fig. 9 VLF anomaly (real and imaginary) along profile P5 and current density section. Dolerite dyke is marked by *dotted green line* and fault/fracture plane is shown by *solid green line*

4.6 Profile P6–P10 (VLF profiles)

To investigate the extension of the fracture seen on profile P5 at 320 m, VLF profiles P6–P10 were conducted further to the north-west. Locations of profiles P6 to P10 are shown in Fig. 3. First, we measured the VLF responses along profile P6 and then moved eastward to profiles P7, P8 and P9. The VLF data were measured up to the maximum possible profile length based on the availability of space and avoiding power line disturbances. Profile P10 was further west of profile P6. The current density sections are combined and are shown in Fig. 10, which indicates good correlation between the various sections, especially fractures (P6—160 m, P7—130 m, P8—120 m, P9—25 m). Profile P9 is very short, but the VLF response depicts the correlating conducting feature at 25 m. The correlating fractures on each profile point towards the Salandi Reservoir in the west and crosscut with the major fracture that is seen on profiles P1, P2 and P5 in the east. Therefore, the Salandi Reservoir could also be a source of water in the OMC mine.

A geophysical survey was not possible in the south-west of the first fracture zone due to the presence of several villages as well as a huge mine dump in this direction. The fracture seen between 150 and 200 m at profile P5 passes below a huge mine dump in the west. Right after the dump, a shallow channel can be seen in Fig. 10. Extension of this shallow channel points towards the river.

4.7 Tracer test (IMFA pond)

After the above-mentioned electrical and electromagnetic studies (P1–P4), the precise location of the fracture was determined and a tracer test was carried out in the IMFA pond. Tracers were pumped within the fracture zone in the IMFA pond. Water samples from different seepage points in the mine were routinely collected and analysed for one year, with an interval of seven days. However, no tracers were observed in the water samples collected from the mine. It has been emphasized that the OMC mine was flooded when the tracer tests were conducted (Dr. A. Mukherjee, Pers. Comm. IIT Kharagpur). In such a situation, collection of water samples from the appropriate locations is the key point of the
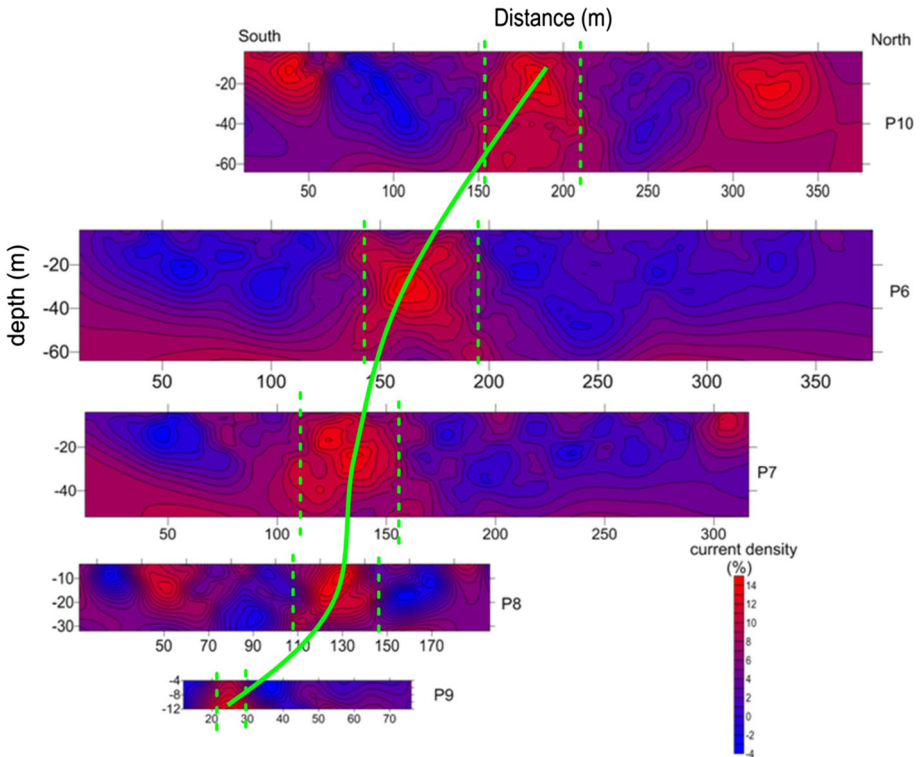
Fig. 10 Apparent current density along profile P6–P10. *Green dotted line* denotes the fracture zone and the *green line* shows its assumed connectivity

tracer test. If samples are not collected from the point of maximum discharge, no signature of the tracer is likely to be noticed. Furthermore, when the tracer is pumped into the open pond, it is rapidly diluted; hence, it is quite likely that the colour was just too diluted to be visible in the mine water.

The absence of tracers in the water samples revealed that either the IMFA pond might not be the actual source of water in the underground OMC mine, or that water samples were not collected at suitable locations. However, it is known that the water in the mine enters from the western side through the delineated fracture. Therefore, VLF measurements were further extended to the west side of the IMFA pond to determine whether distant sources such as the Salandi River and the Salandi Reservoir could be the possible sources of water in the mine.

The water samples collected from the seepage points, IMFA, OMC ponds, groundwater and reservoir samples show the same concentration of Ca^{2+} and HCO_3^-. Also, the cation concentrations present within the IMFA and OMC ponds are different to the seepage water, which has low cation concentrations, dominated by Ca. This suggests that the seepage water, groundwater and reservoir water are approximately situated at the same position, whereas IMFA pond water and OMC pond water are away. Hence, seepage water is distinct from the OMC and IMFA pond water, but it is similar to groundwater and reservoir water.

4.8 Tracer test (borehole)

To test whether the Salandi Reservoir is a source of water in the OMC mine, a 30-m-deep tube well was drilled exactly over the fracture on profile P8. The lithology of the 30-m-deep vertical borehole conducted for the hydrological test at location N-21°16′11.1″ E-86°19′22.0″ consists primarily of weathered ortho-pyroxenite and serpentine. Water was encountered at a depth of 4.5 m onwards. This reveals that water in this area flows through an unconfined aquifer.

The lithology correlated very well with the interpreted current density section. A conductive feature extending to a depth of 30 m was observed at a distance of about 25 m along profile P8 (Fig. 11). The presence of water in this borehole at high pressure (which resulted in a water level rise to only 4.5 m) suggests that water is also present along the delineated fractures in other profiles.

To establish these geophysical findings, a tracer test was conducted through this borehole. However, the tracer was once again not detected in water samples collected from the OMC mine. This was because if pond is the source of water in the mine, then water level in pond will decrease rapidly; however, this is not the case. Water in IMFA pond remains in large volume and decreases slowly. Therefore, this pond alone cannot be the source of water in the mine.

The geophysical survey predicted the location and direction of the fracture, and the drilled borehole proves that the fracture was filled with water at high pressure. However, whether water flowing through this fracture is the source of the water in the OMC mine can only be established by hydrogeological testing. Water pressure increases with depth; as a result, if the tracer in the well is not forced to pass into the subsurface, then it will remain in the borehole, causing the hydrogeological test to fail. Two hydrogeological tracer tests were conducted, but the tracer could not be detected in the mine. This means that the water entering the mine is either natural groundwater seeping into the area or moving through the main fracture. However, the fact remains that water enters the mine from the west and will
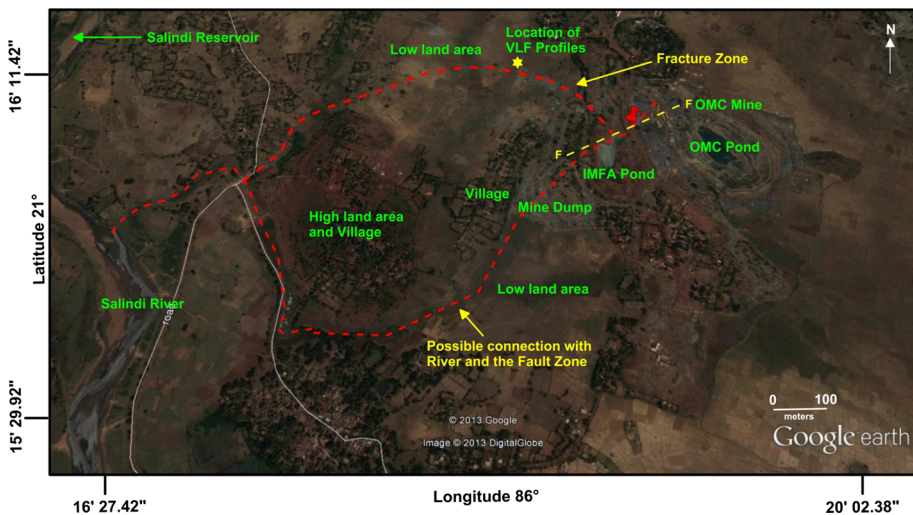

Fig. 11 Google earth image showing low land and possible connection with river of the delineated fracture at VLF profiles

continue to pose a problem unless a suitable dewatering mechanism is implemented to intercept the water before it enters the mine.

5 Conclusions

Geophysical survey using VLF electromagnetic, resistivity and SP measurements was carried out to delineate the source of the water influx in an underground Bangur chromite mine. Geophysical surveys conducted west of the mine inferred the extent of a major fracture zone. The delineated fracture zone correlates with a fracture zone seen in the underground mine. The study confirms that this fracture zone passes through the IMFA pond and further extends in a western direction beyond the IMFA pond towards the Salandi River, as well as the Salandi Reservoir. Correlations of a fracture zone depicted on various VLF profiles suggest that the fracture extends towards the Salandi Reservoir. Furthermore, a linear trending shallow zone (low land area) following the IMFA mine dump pointed towards the Salandi River. Thus, the IMFA pond, the Salandi River and the Salandi Reservoir may all be sources of the water in the mine. So far, hydrogeological tracer studies conducted at two potential delineated fracture locations failed to prove the source of the water. Regardless of whether further hydrogeological studies establish this or not, we recommend that a 30- to 40-m-deep (vertical/slanting) tube well be drilled exactly in the fracture plane depicted in the VLF profile adjacent to the IMFA pond and that the maximum possible amount of water be pumped to dewater the fracture zone before it enters the mine for safety in mining operations. If pumped water will be dumped into the nearby pond (IMFA or other dump ponds), then it will re-enter in the mine through interconnected minor fracture. Therefore, to avoid this, pumped water should be dumped in the canal which is about 2.5 km from the mine so that the same water can be used for agricultural purpose.

References

Banerjee PK (1972) Geology and geochemistry of the Sukinda ultramafic field, Cuttack district, Orissa. Mem Geol Surv India 103:171

Biswas A, Sharma SP (2015) Can very low frequency electromagnetic survey detect graphite deposits in the subsurface? Initial results from Daltanganj, Jharkhand, India. J Geol Soc India 86(5):530–534

Dhal B, Das NN, Pandey BD, Thatoi HN (2011) Environmental quality of the Boula-Nuasahi chromite mine area in India. Mine Water Environ 30:191–196

Jakubick A, Jenk U, Kahnt R (2002) Modelling of mine flooding and consequences in the mine hydrogeological environment: flooding of the Koenigstein mine, Germany. Environ Geol 42(2–3):222–234

Karous M, Hjelt SE (1983) Linear-filtering of VLF dip-angle measurements. Geophys Prospect 31:782–894

Klapper H, Geller W, Schultz M (1996) Abatement of acidification in mining lakes in Germany. Lakes Reserv Res Manag 2(1–2):7–16

Landerarbeitsgemeinschaft Wasser [LAWA] (2001) Tagebaurestseen-Anforde-rungenan die Wasserqualitat. Kulturbuch-Verlag, Berlin

Moebs NM, Sames GP (1989) Water—a hazard and a nuisance. Coal 26(10):60–63

Mohanty WK, Mandal A, Sharma SP, Gupta S, Misra S (2011) Integrated geological and geophysical studies for delineation of chromite deposits: a case study from Tangarparha, Orissa, India. Geophysics 76(5):1–13

Nuttall CA, Younger PL (2004) Hydrogeochemical stratification in flooded underground mines: an overlooked pit. J Contam Hydrol 69:101–114

Ricka A, Kuchovsky T, Sracek O, Zeman J (2010) Determination of potential mine water discharge zones in crystalline rocks at Rozna, Czech Republic. Environ Earth Sci 60(6):1201–1213

Saha AK (1994) Crustal evolution of Singhbhum North Orissa, Eastern India. Geol Soc India Memoir 27:341

Sahoo KC, Mohanty M, Sahoo P, Rath SC, Ray SB (2014) Occurrence of PGE mineralisation in Bangur, Kendujhar district, Odisha. J Geol Soc India 83:31–37

Sharma SP, Baranwal VC (2005) Delineation of groundwater-bearing fracture zones in a hard rock area integrating very low frequency electromagnetic and resistivity data. J Appl Geophys 57:155–166

Sharma SP, Biswas A, Baranwal VC (2014) Very low frequency electromagnetic method—a shallow subsurface investigation technique for geophysical applications. In: Sengupta D (ed) recent trends in modeling of environmental contaminants. Springer, Dordrecht

Sui W, Liu J, Yang S, Chen Z, Hu Y (2011) Hydrogeological analysis and salvage of a deep coalmine after a groundwater inrush. Environ Earth Sci 62(4):735–749

Telford WM, Geldart LP, Sheriff RE (1990) Applied geophysics. Cambridge University Press, Cambridge

Vutukuri V, Singh R (1995) Mine inundation-case histories. Mine Water Environ 14(annual issue):107–130

Wanfang Z (1997) Karst water control and management in the Hanxing mining area of North China. Environ Geol 30:280–284